



Evaluation of BDE-47-induced neurodevelopmental toxicity in zebrafish embryos

Juan Zhuang¹ · Zheng-jun Pan¹ · Ying Qin¹ · Hui Liang¹ · Wen-feng Zhang¹ · Ze-yu Sun¹ · Han-bo Shi¹

Received: 2 August 2022 / Accepted: 23 February 2023 / Published online: 4 March 2023
© The Author(s), under exclusive licence to Springer-Verlag GmbH Germany, part of Springer Nature 2023

Abstract

There are growing concerns about the neurodevelopmental toxicity of polybrominated diphenyl ethers (PBDEs), but the toxicological phenotypes and mechanisms are not well elucidated. Here, zebrafish (*Danio rerio*) were exposed to 2,2',4,4'-tetrabromodiphenyl ether (BDE-47) from 4 to 72 h post-fertilization (hpf). The results showed that BDE-47 stimulated the production of dopamine and 5-hydroxytryptamine, but inhibited expression of Nestin, GFAP, Gap43, and PSD95 in 24 hpf embryos. Importantly, we unraveled the inhibitory effects of BDE-47 on neural crest-derived melanocyte differentiation and melanin syntheses process, evidenced by disrupted expression of *wnt1*, *wnt3*, *sox10*, *mitfa*, *tyrp1a*, *tyrp1b*, *tryp2*, and *oca2* gene in 72 hpf embryos and decreased tyrosinase activities in embryos at 48 and 72 hpf. The transcriptional activities of *myosin VAa*, *kif5ba*, *rab27a*, *mlpha*, and *cdc42* genes, which are associated with intracellular transport process, were also disturbed during zebrafish development. Ultimately, these alterations led to fast spontaneous movement and melanin accumulation deficit in zebrafish embryos upon BDE-47 exposure. Our results provide an important extension for understanding the neurodevelopmental effects of PBDEs and facilitate the comprehensive evaluation of neurotoxicity in embryos.

Keywords Polybrominated diphenyl ethers · Zebrafish · Neurotoxicity · Melanin pigmentation

Introduction

For decades, polybrominated diphenyl ethers (PBDEs) have been extensively applied as additive brominated flame retardants in commercial products including electronics, appliances, textiles, and household furnishing. Although many PBDEs have been banned or voluntarily phased out in the USA and European countries, large amounts of in-use consumer products and environmental reservoirs containing PBDEs still exist (Cai et al. 2022). It has been estimated that the total consumption of penta-, octa-, and deca-BDE was ~46,000, ~25,000, and ~380,000 tonnes, respectively, in 35 products considered in the USA and Canada from 1970 to

2020 (Abbasi et al. 2015). Indeed, high concentrations of PBDEs were widely detected in environmental media (Lin et al. 2022). In soil and road dust samples, PBDE concentrations ranged from 0.13 to 590 ng/g, dw, and 3.3–600 ng/g, dw, respectively (Li et al. 2018); the highest PBDE concentration (390,000 ng/g dw) was detected in a sample from an e-waste open-burning site (Labunska et al. 2013). Hou et al. (2019) detected the water, sediment, and fish samples from the Jinjiang River (Chengdu, China) and found the BDE-47 concentrations were 0.25 ng/L, 0.29 ng/g, dw, and 9.5–15.8 ng/g, lw, respectively. Maximum PBDE concentration (18,000 ng/g lw) has been found in the eggs of peregrine falcons (*Falco peregrinus*) (Lindberg et al. 2004). Labunska et al. (2014) estimated that the median PBDE exposure levels around e-waste recycling sites were 130.9 and 614.1 ng/kg bw/day for adults and children, respectively.

Prenatal or neonatal exposure to PBDEs has been associated with complex neurotoxicity outcomes in children, such as slower neuropsychological development (Drobná et al. 2019), lower levels of social and language development (Ding et al. 2015), poorer fine motor skills (Eskenazi et al. 2013), neurobehavioral abnormalities (Ji et al. 2019a), lower cognitive ability (Azar et al. 2021), and reading skills

Responsible Editor: Bruno Nunes

✉ Juan Zhuang
dajiangsky@163.com

¹ Jiangsu Key Laboratory for Eco-Agricultural Biotechnology Around Hongze Lake, Jiangsu Collaborative Innovation Center of Regional Modern Agriculture and Environmental Protection, Jiangsu Engineering Laboratory for Breeding of Special Aquatic Organisms, Huaiyin Normal University, 111 Changjiang West Road, Huaian 223300, Jiangsu, China

(Liang et al. 2019). In animal studies, neurotoxic effects of PBDEs were mainly manifested as altered spontaneous behavior and cognitive deficits (Liu et al. 2022; Zheng et al. 2021; Blanc et al. 2021; Dingemans et al. 2007), and perturbation of thyroid hormone homeostasis, oxidative stress-induced damage, interference with signal transduction, and disruption of neurotransmitter systems were suggested to be the potential mechanisms (Blanco et al. 2013; Costa et al. 2015; Chen et al. 2018; Dingemans et al. 2007). Although the neurodevelopmental effects of PBDEs have been extensively explored, the neurotoxicity phenotypes and the underlying mechanisms have not been completely elucidated.

2,2',4,4'-tetrabromodiphenyl ether (BDE-47) is a prominent PBDE congeners, accounting for above 50% of the total PBDEs in maternal or placental serum (Azar et al. 2021; Varshavsky et al. 2020). Zebrafish is a favorable in vivo model for studying neurotoxicity of PBDEs (Zheng et al. 2021). Zebrafish tail coiling is sensitive to chemical stimulus, which has been extensively taken as a useful behavioral endpoint of neurodevelopmental toxicity (Zheng et al. 2021). In our pilot study, BDE-47 increased tail coiling but reduced skin melanin accumulation in zebrafish embryos. Melanocytes are pigment-producing cells originated from neural crest cells, and melanocyte generating was related to the development of nervous system (Yaar and Park, 2012; Wang et al. 2020). Thereby, changes in embryonic neurobehavior and skin pigmentation following BDE-47 exposure were monitored; biochemical indicators such as monoaminergic neurotransmitter content, melamine content, and tyrosinase activity were detected; and genes or protein expression that are responsible for nervous system development, melanocyte development, melanin syntheses, and intracellular transport process were analyzed in zebrafish embryos. Our results will enrich our understanding of neurodevelopmental toxicity of PBDEs and facilitate the comprehensive evaluation of neurotoxicity in embryos.

Materials and methods

Chemicals and reagents

BDE-47 (> 99%) was purchased from ChemService, West Chester, PA. It was dissolved in DMSO (> 99.9%; Sigma-Aldrich, St. Louis, MO) and diluted to 1.250, 0.625, or 0.312 mg/L by adding zebrafish embryo culture medium (5 mM NaCl, 0.33 mM MgSO₄, 0.33 mM CaCl₂, and 0.17 mM KCl; pH7.2–7.4; Nanjing EzeRinka Biotechnology Co., Ltd., China). The TRIzol reagent was purchased from Invitrogen (Carlsbad, CA, USA). The reverse transcription kit and SYBR Green Master Mix were purchased from Takara (Dalian, China). Melamine, L-DOPA, and mushroom tyrosinase were from Sigma-Aldrich.

Zebrafish TyR ELISA kit, Dopamine ELISA kit, and 5-HT ELISA kit were obtained from enzyme-linked Biotechnology (Shanghai, China). Antibody against Mitfa was obtained from GeneTex (North America). Antibodies against Nestin, growth-associated protein 43 (Gap43), postsynaptic density protein 95 (PSD95), glial fibrillary acidic protein (GFAP) and glyceraldehyde-3-phosphate dehydrogenase (GAPDH), horseradish peroxidase (HRP) conjugated goat anti-rabbit IgG, and fluorescein (FITC)-conjugated anti-rabbit IgG were obtained from Proteintech Group (China). Primer sequences were synthesized by Sangon Biotech Co., Ltd. (Shanghai, China).

Fish husbandry and embryo collection

Adult AB strain zebrafish (*Danio rerio*) were purchased from Nanjing EzeRinka Biotechnology Co., Ltd. (Nanjing, China). Zebrafish were maintained in fish water (pH 7.4–7.8, conductivity 450–550 µS/cm) at 28 °C with a 14 h light and 10 h dark lighting schedule and fed with freshly hatched brine shrimp. Male and female zebrafish were placed into the spawning boxes overnight at a ratio of 1:1. Embryos were collected within 30 min after spawning and incubated in embryo medium at 28 °C.

BDE-47 exposure

BDE-47 exposure concentrations were chosen according to the previous work of Tanaka et al. (2018) and our pilot study. 6-well cell culture plates (Corning Inc. Steuben, New York, USA) were used in the experiments. The plates were incubated with the respective concentrations of BDE-47 24 h before embryo exposure. Then embryos were randomly divided into 6-well plates with about 50 embryos per well, and then exposed to 6 mL BDE-47 solutions (0, 0.325, 0.625, or 1.250 mg/L; DMSO, < 0.03%) with a minimum of three replicates. Our pilot experiment suggested that 0.03% v/v DMSO had no negative effect on embryo development. The exposure period was from 4 to 72 h post-fertilization (hpf). The incubating conditions for the embryos were the same as those for the adult fish. The exposure solution was renewed every day.

Spontaneous movement

At 24 hpf, the movements of embryos were monitored using a CCD camera (Optec TP310, China) connected to the stereomicroscope (Optec SZ780, China) as the previous report (Ramlan et al. 2017). Coiling movement is a full-body contraction that brings the tip of the tail to the head. The number of spontaneous movement and tail coiling of the zebrafish embryos without morphological malformations was counted within a 1-min period.

Morphological skin pigmentation and melanin analysis

The morphological skin pigmentation was checked using a stereomicroscope (Optec SZ780, China), and images were taken using a CCD camera (Optec TP310, China). The areas of skin melanosomes covering the dorsal regions of the zebrafish head and yolk sac and excluding the dark area covered by eyes were quantified at 72 hpf using the software image-pro plus according to the previous study (Burgoyne et al. 2015). The threshold setting in image-pro plus was used to remove all image information excluding melanosomes, allowing measurement of melanin area.

The melanin content was measured in 72 hpf embryos as described by Wang et al. (2020). Briefly, 50 zebrafish embryos of each group were anesthetized with MS-222 (0.016%) and homogenized in ice-cold phosphate buffers (PBS) and centrifuged at 10,000 rpm for 20 min at 4 °C ($n = 3$). After centrifugation, the melanin precipitation was resuspended with 1N NaOH/10% DMSO and vortexed. The mixture was incubated at 95 °C in dark to solubilize the melanin for 10 min. The absorbance at 405 nm was measured using a microplate reader, and the zebrafish embryonic melanin content was determined from a standard curve prepared from an authentic standard of synthetic melanin.

Tyrosinase activity assay

After anesthetization with MS-222 (0.016%), zebrafish embryos (50 embryos of each group) at 48 hpf ($n = 5$) or 72 hpf ($n = 4\sim 5$) were homogenized in ice-cold PBS and centrifuged at 10,000 rpm for 20 min at 4 °C. The supernatants' solution was used for zebrafish tyrosinase activity determination according to the manufacturer's instructions of the zebrafish TyR ELISA kit. Briefly, standard or samples (50 μ L) and HRP conjugate (100 μ L) were added to standard wells and sample wells and incubated at 37 °C for 1 h. Then, the incubation mixture was removed and washed with PBS four times. A total of 100 μ L 3, 3', 5, 5'-tetramethylbenzidine (TMB) substrate was added to each well and incubated for 15 min at 37 °C. Finally, stop solution H₂SO₄ (50 μ L) was added to each well, and the absorbance was measured at 450 nm. The tyrosinase activity was determined by comparing the standard curve.

To determine whether BDE-47 can directly inhibit tyrosinase activity, mushroom tyrosinase and L-DOPA were used according to the L-DOPA chrome formation method (Liu et al. 2019). Briefly, 50 μ L solvent control or BDE-47 (0.325, 0.625, or 1.250 mg/L) was mixed with 50 μ L mushroom tyrosinase solution (700 U/mL) and 100 μ L PBS (0.1 mol/L, pH 6.8). A total of 100 μ L L-DOPA (5 mM) was used as substrate and added into the mixture ($n = 3$). The mixture

was incubated for 20 min at 37 °C, and the absorbance value of the dopachrome product was measured at 475 nm.

Measurement of monoaminergic neurotransmitters

After anesthetization with 0.016% MS-222, zebrafish embryos (50 embryos of each group, $n = 4$) at 24 hpf were homogenized in ice-cold PBS and centrifuged at 10,000 rpm for 20 min at 4 °C. The supernatants of zebrafish embryos at 24 hpf were used to examine the concentrations of 5-hydroxytryptamine (5-HT) or dopamine according to the manufacturer's instructions of the zebrafish dopamine or 5-HT ELISA kit. Briefly, standard or samples (50 μ L) and HRP conjugate (100 μ L) were added to standard wells and sample wells of dopamine or 5-HT ELISA kit and then incubated for 1 h at 37 °C. After being washed with PBS four times, 100 μ L TMB solution was added to each well and incubated for 15 min at 37 °C. Finally, H₂SO₄ (50 μ L) was added to each well as a stop solution, and the absorbances at 450 nm were measured. The dopamine or 5-HT concentrations were determined from the standard curve.

Real-time PCR

Zebrafish total RNAs (30 embryos of each group, $n = 3$) were extracted using TRIzol Reagent. cDNA was synthesized using cDNA reverse transcription kits. SYBR-Green quantitative PCR analysis was performed using an SYBR Green Master Mix and the Bio-Rad CFX96 Real-Time System (Hercules, CA, USA). Expression of *wnt1*, *wnt3*, *sox10*, *mitfa*, *tyrp1a*, *tyrp1b*, *tryp2*, *oca2*, *myosin VAA*, *kif5ba*, *rab27a*, *mlpha*, and *cdc42* were detected. The primer sequences are presented in Supplementary Table 1.

Western blot

The protein samples (40 μ g protein/sample, $n = 3$) were separated using 10% sodium dodecyl sulfate-polyacrylamide gelelectrophoresis (SDS-PAGE) and transferred to polyvinylidene difluoride membrane. Next, the membranes were blocked with 1 \times TBST with 5% nonfat dried milk for 1 h and then incubated with primary antibodies overnight at 4 °C. After being washed with TBST three times, the membranes were incubated with peroxidase-conjugated secondary antibody for 1 h at 22 °C and visualized using enhanced chemiluminescence.

Whole-mount immunofluorescence staining

Zebrafish embryos were fixed with 4% paraformaldehyde at 4 °C for 4 h. After being permeabilized by 100% methanol, embryos were incubated with Nestin antibody at 4 °C overnight. Subsequently, FITC-conjugated anti-rabbit IgG was applied after washing in PBS.

Statistical analysis

All the experiments were performed in triplicate, and the results were expressed as the mean \pm standard error. Statistical analysis was performed with one-way ANOVA followed by Dunnett's Multiple Comparison Test using GraphPad Prism 5.0 software. A P value of < 0.05 was considered statistically significant.

Results

Spontaneous movement and morphological observation

Zebrafish coiling movement is regarded as a rapid and sensitive endpoint for neurotoxicity evaluation (Wang et al. 2018; Zheng et al. 2021). Previous reports demonstrated that BDE-47 stimulated zebrafish coiling activity, but the triggering concentrations were inconsistent (Usenko et al. 2011; Tanaka et al. 2018). We treated embryos with BDE-47 and observed the spontaneous movement at 24 hpf. As shown in Fig. 1, zebrafish spontaneous movement was stimulated by BDE-47 at 1.250 mg/L (Fig. 1a; $P < 0.05$, versus control group), and the coiling frequency was increased (Fig. 1b, $P < 0.01$, versus control group).

In addition to the neurobehavioral changes in 24 hpf embryos, further observation of the developing embryos revealed a novel effect of BDE-47 manifested in the suppression of skin pigmentation. As shown in Fig. 2, notable skin pigmentation appeared in the embryonic head, abdomen, and dorsolateral trunk from 32 hpf onward. Melanosomes in the skin covering the head, yolk sac, and notochord significantly were significantly suppressed in embryos starting from 32 hpf due to BDE-47 exposure concentration-dependently. The presented data indicated that BDE-47 disrupted skin pigmentation in zebrafish embryos.

Concentrations assays of 5-HT and dopamine

Dopamine and 5-HT play vital roles in zebrafish central nervous system development, behavior, and movement (Brustein et al. 2003; Thirumalai and Cline, 2008). Thus, we assessed whether the concentrations of 5-HT and dopamine changed in zebrafish exhibiting increased coiling at 24 hpf. As shown in Fig. 3a, 1.250 mg/L BDE-47 increased 5-HT levels ($P < 0.05$, versus control group), and the contents of dopamine were also elevated (Fig. 3b, $P < 0.05$, versus control group).

Melanosome area, melanin content and tyrosinase activity

To quantify the melanin presence, skin melanosome areas within the defined dorsal regions of the head and yolk sac (Fig. 4a) and melanin contents were measured in 72 hpf zebrafish. Results showed that zebrafish melanosome areas were markedly reduced in 0.625 and 1.250 mg/L BDE-47 groups (Fig. 4a, BDE-47_{0.625 mg/L}: $P < 0.05$; BDE-47_{1.250 mg/L}: $P < 0.01$, versus control group), and the melanin contents were accordingly decreased (Fig. 4b, BDE-47_{0.625 mg/L}: $P < 0.05$; BDE-47_{1.250 mg/L}: $P < 0.001$, versus control group). Furthermore, the effect of BDE-47 on tyrosinase activity was investigated, and the results suggested BDE-47 inhibited tyrosinase activities in zebrafish embryos at 48 and 72 hpf (Fig. 4c; embryos at 48 hpf: BDE-47_{0.625 mg/L}: $P < 0.01$; BDE-47_{1.250 mg/L}: $P < 0.001$; Fig. 4d; embryos at 72 hpf: BDE-47_{0.625 mg/L}: $P < 0.05$; BDE-47_{1.250 mg/L}: $P < 0.001$, versus control group). However, BDE-47 did not affect the enzymatic activities of mushroom tyrosinase at all concentrations in vitro test (Fig. 4e, $P > 0.05$, versus control group).

Fig. 1 BDE-47 altered spontaneous movement behavior in zebrafish embryos at 24 hpf. Zebrafish embryos were exposed to various concentrations of BDE-47 beginning at 4 hpf. **a** Zebrafish embryonic spontaneous movement. **b** Zebrafish embryonic coiling activities. ($n = 25$). * $P < 0.05$, ** $P < 0.01$ versus control group

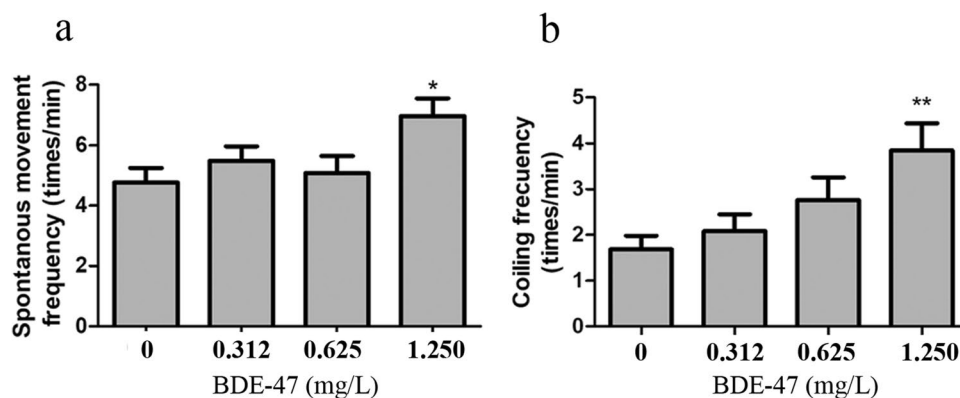


Fig. 2 Effects of BDE-47 on morphological color change of zebrafish embryos. Zebrafish embryos were exposed to various concentrations of BDE-47 beginning from 4 to 72 hpf. The morphological skin pigmentation was observed under the stereomicroscope at 32 hpf, 48 hpf, or 72 hpf

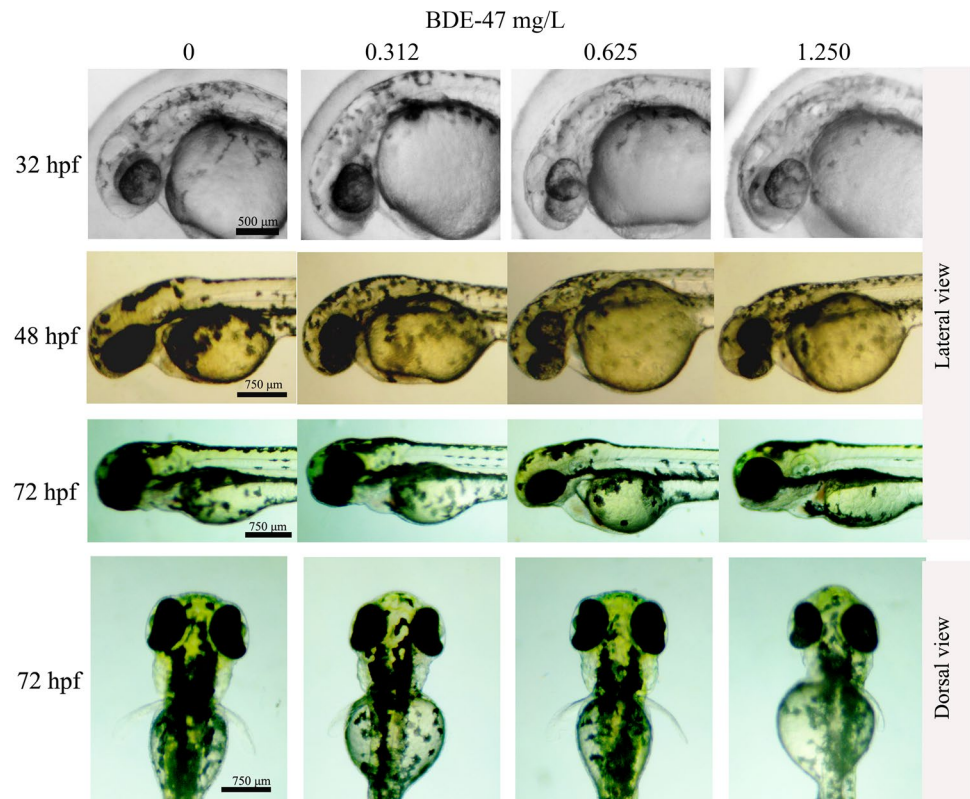
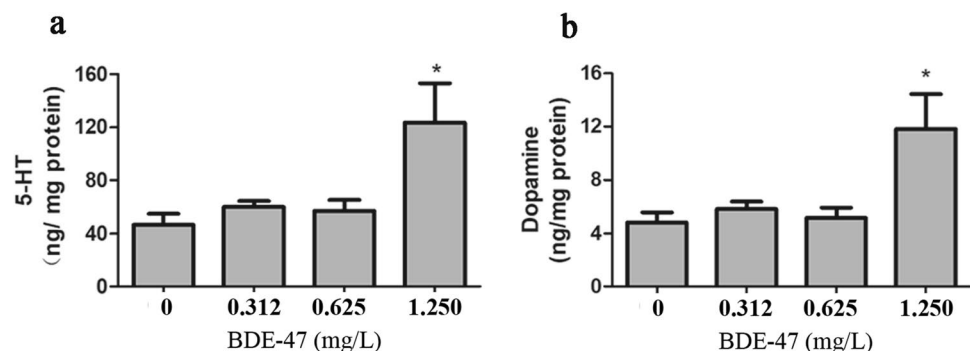


Fig. 3 Concentrations of 5-HT and dopamine were increased by BDE-47 in zebrafish embryos at 24 hpf. Zebrafish embryos were exposed to various concentrations of BDE-47 beginning at 4 hpf. **a** 5-HT concentrations. **b** Dopamine concentrations. ($n = 4$). * $P < 0.05$ versus the control group



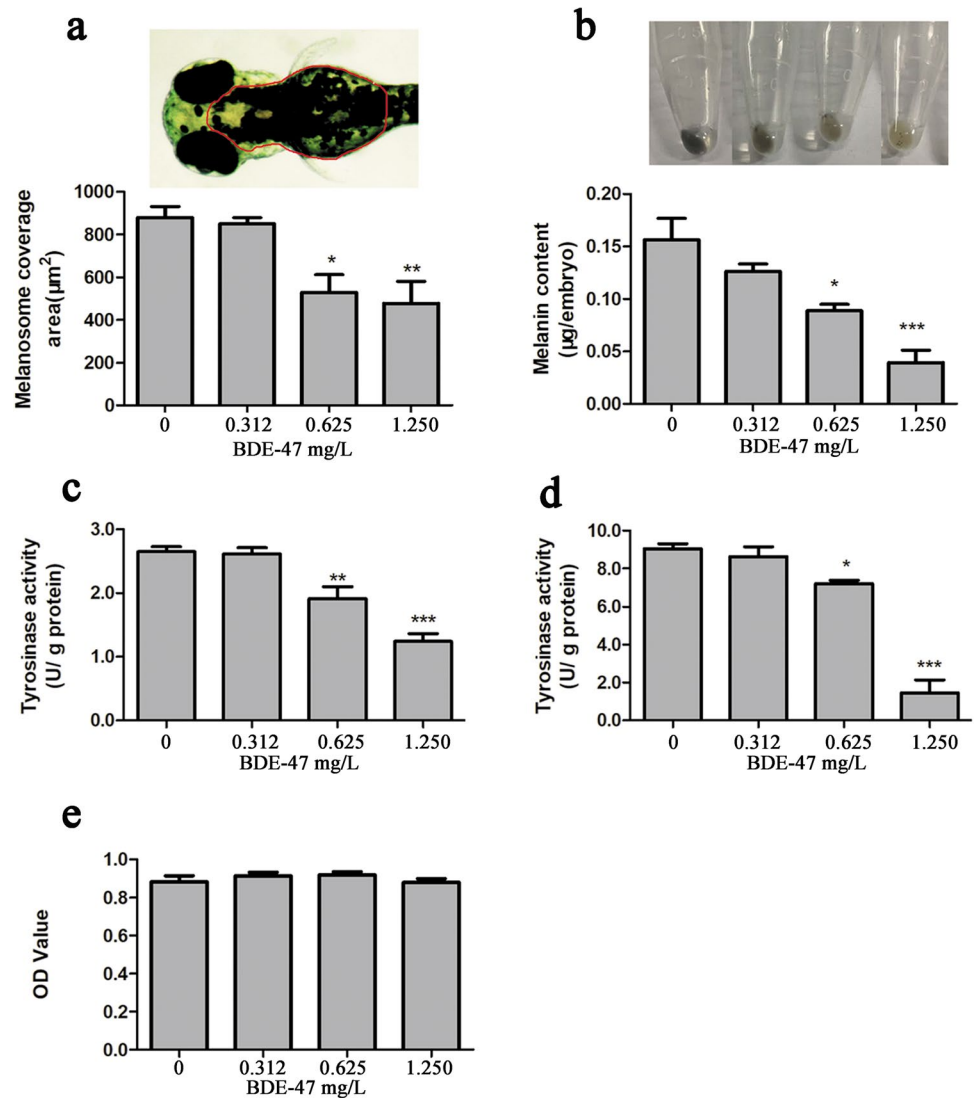
Proteins expression related to neural development

We further analyze the protein expression related to neural development in 24 hpf BDE-47-treated embryos. As shown in Fig. 5a and b, BDE-47 significantly inhibited the expression of Nestin, PSD95, and GFAP at concentrations of 0.625 and 1.250 mg/L (Nestin: BDE-47_{0.625 mg/L}: $P < 0.01$; BDE-47_{1.250 mg/L}: $P < 0.05$; PSD95: $P < 0.05$; GFAP: BDE-47_{0.625 mg/L}: $P < 0.05$; BDE-47_{1.250 mg/L}: $P < 0.01$; versus control group), and decreased the protein level of Gap43 at 1.250 mg/L ($P < 0.05$, versus control group). Immunofluorescence staining results suggested that Nestin protein was widely expressed in the embryonic brain at 24 hpf, and the positive signal intensity was decreased by BDE-47 (Fig. 5c).

Expression of genes or proteins related to skin melanocyte differentiation and melanogenesis

Gene expression related to melanocyte differentiation and melanogenesis in zebrafish embryos at 72 hpf was analyzed. Gene expression of wingless-type MMTV integration site family member 1 (*wnt1*) and member 3a (*wnt3a*), which are responsible for melanocyte differentiation, were significantly inhibited at all BDE-47 tested concentrations (Fig. 6a, *wnt1*: BDE-47_{0.312 mg/L}: $P < 0.05$; BDE-47_{0.625 mg/L} and BDE-47_{1.250 mg/L}: $P < 0.001$; Fig. 6b, *wnt3a*: $P < 0.001$; versus control group). The transcriptional level of SRY-Box transcription factor 10 (*sox10*) was decreased in 0.625 or 1.250 mg/L BDE-47 group (Fig. 6c, BDE-47_{0.625 mg/L}: $P < 0.001$; BDE-47_{1.250 mg/L}: $P < 0.01$; versus

Fig. 4 Effects of BDE-47 on skin melanosome area, melanin content, and tyrosinase activity. Zebrafish embryos were exposed to various concentrations of BDE-47 beginning from 4 to 72 hpf. **a** Melanosome areas within the defined region of zebrafish embryos (indicated red-outlined area, the dorsal regions of the head and yolk sac of zebrafish) at 72 hpf were quantified using the software image-pro plus ($n = 5-6$). **b** A schematic representation of melanin extracted from zebrafish embryos and melanin contents of zebrafish embryos at 72 hpf ($n = 3$). **c** Embryonic tyrosinase activities at 48 hpf ($n = 5$). **d** Embryonic tyrosinase activities at 72 hpf ($n = 4-5$). **e** Mushroom tyrosinase activities ($n = 3$). * $P < 0.05$, ** $P < 0.01$, *** $P < 0.001$ versus control group



control group). The expression of melanocyte-inducing transcription factor a (*mitfa*) was reduced in 0.312 mg/L or 1.250 mg/L BDE-47 group, while increased in 0.625 mg/L BDE-47 group (Fig. 6d, BDE-47_{0.312 mg/L}: $P < 0.05$; BDE-47_{0.625 mg/L} and BDE-47_{1.250 mg/L}: $P < 0.01$; versus control group). Tyrosinase-related protein (*tyrp*) and oculocutaneous albinism II (*oca2*) are involved in melanin biosynthesis, and *tyrp1a* was transcriptionally up-regulated in 0.625 mg/L BDE-47 group (Fig. 6e, $P < 0.01$; versus control group), while the expression of *tyrp1b*, *tryp2*, and *oca2* genes were significantly inhibited by BDE-47 (Fig. 6f, *tyrp1b*: BDE-47_{0.312 mg/L-1.250 mg/L}: $P < 0.001$; Fig. 6g, *tryp2*: BDE-47_{0.312 mg/L-1.250 mg/L}: $P < 0.001$; Fig. 6h, *oca2*: BDE-47_{0.625 mg/L} and BDE-47_{1.250 mg/L}: $P < 0.01$; versus control group). Western blot analysis results showed BDE-47 decreased protein expression of *mitfa* in 72 hpf embryos at concentrations of 0.625 and 1.250 mg/L (Fig. 6i, $P < 0.001$; versus control group). These findings suggested that BDE-47

may disrupt the process of melanocyte differentiation and melanogenesis.

Gene expression associated with the intracellular transport process

Motor-dependent intracellular transport is required for cell polarity and function in nerve cells and melanocytes (Ultanir et al. 2014; Edgar and Bennett, 1999). Thus real-time PCR analysis was performed to determine the effects of BDE-47 on actin- and microtubule-dependent transport. At 24 hpf, BDE-47 stimulated the expression of actin-based processive motor *myosin VAa* in zebrafish embryos at concentrations of 0.312 mg/L and 1.250 mg/L (Fig. 7a, $P < 0.01$; versus control group), while the expression of microtubule-associated motor kinesin family member 5b (*kif5b*)a was not significantly affected (Fig. 7b, $P > 0.05$; versus control group). Besides, gene expression of *mlpha*, *rab27a*,

Fig. 5 Effects of BDE-47 on protein expression related to neural development at 24 hpf. Zebrafish embryos were exposed to various concentrations of BDE-47 beginning at 4 hpf. **a** Representative images of protein expression of Nestin, Gap43, PSD95, GFAP, and GAPDH. **b** The relative densitometry analysis of Nestin, GAP43, PSD95, and GFAP (normalized to GAPDH) ($n = 3$). **c** Representative images of Nestin immunofluorescence staining. FITC was used to visualize the nestin positive signal (green). * $P < 0.05$, ** $P < 0.01$ versus control group

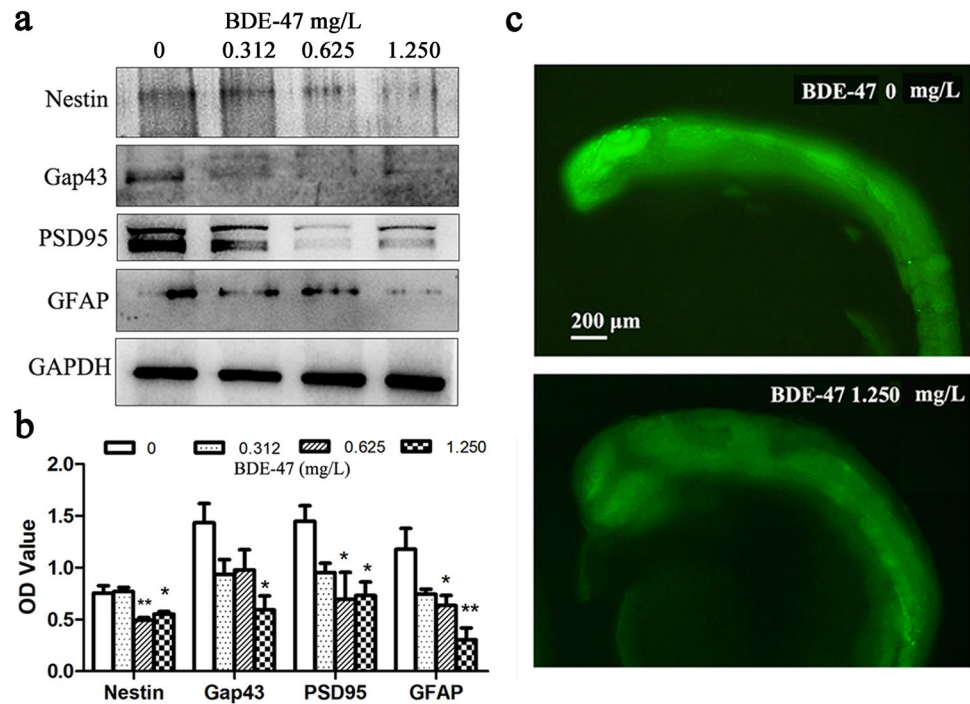
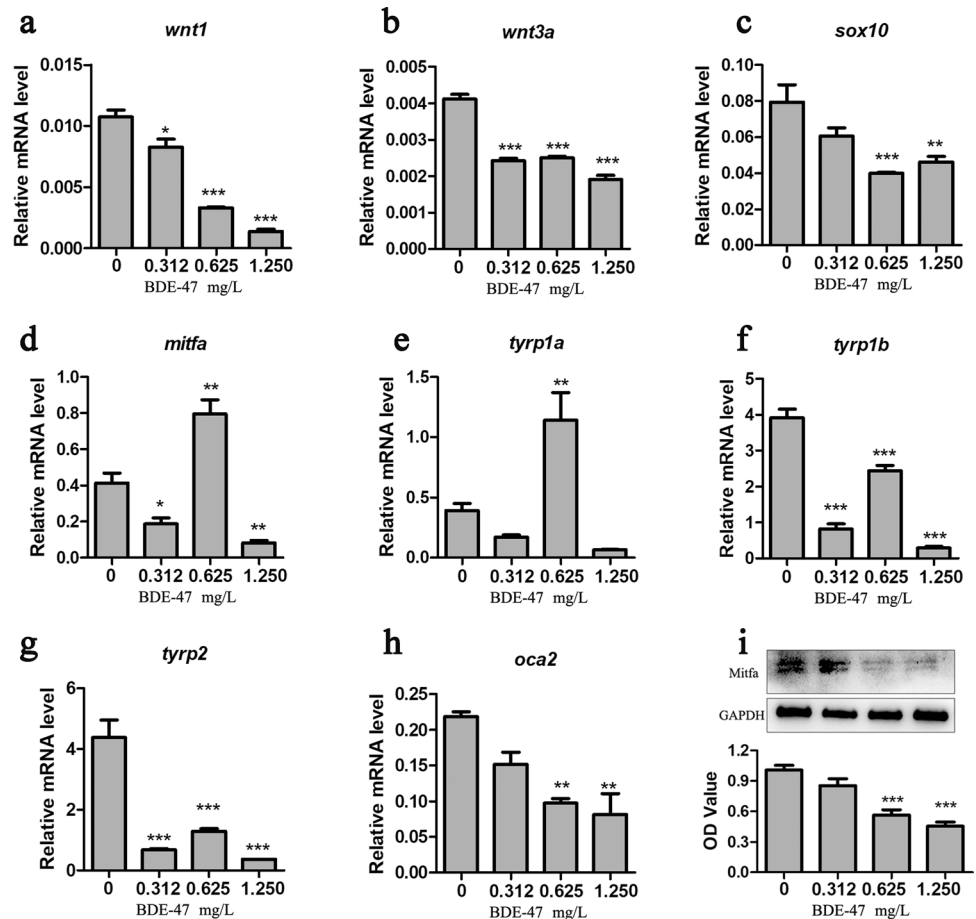


Fig. 6 Effects of BDE-47 on melanocyte differentiation and melanogenesis in zebrafish embryos at 72 hpf. Zebrafish embryos were exposed to various concentrations of BDE-47 beginning at 4 hpf. **a–h** Analysis of the gene expression of *wnt1*, *wnt3a*, *sox10*, *mitfa*, *tyrp1a*, *tyrp1b*, *tyrp2*, and *oca2* (normalized to β -actin). **i** Immunoblotting and densitometry analysis of Mitfa. The relative densities were expressed as the ratio of Mitfa to GAPDH. ($n = 3$). * $P < 0.05$, ** $P < 0.01$, *** $P < 0.001$ versus control group



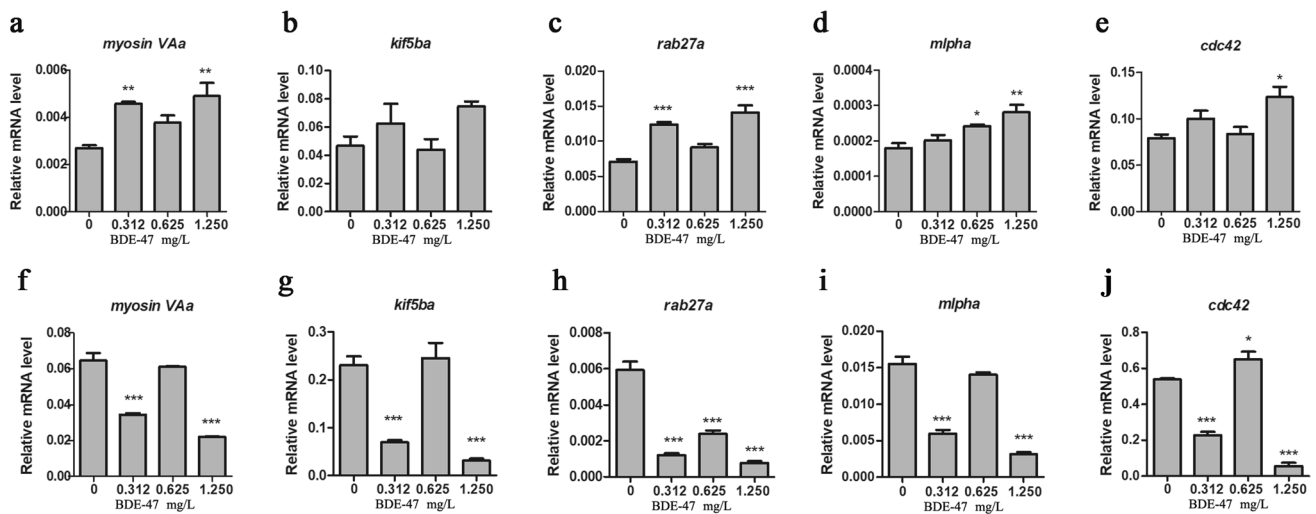


Fig. 7 Effects of BDE-47 on gene expression associated with intracellular transport process in 24 hpf and 72 hpf zebrafish embryos. Zebrafish embryos were exposed to various concentrations of BDE-47 beginning from hpf to 72 hpf. **a–e** Analysis of the gene expression of *myosin VAa*, *kif5ba*, *rab27a*, *mlpha*, and *cdc42* in 24 hpf zebrafish

embryos (normalized to β -actin). **f–j** Analysis of the gene expression of *myosin VAa*, *kif5ba*, *rab27a*, *mlpha*, and *cdc42* in 72 hpf zebrafish embryos (normalized to β -actin). ($n = 3$). * $P < 0.05$, ** $P < 0.01$, *** $P < 0.001$ versus control group

and *cdc42* was increased due to BDE-47 exposure (Fig. 7c, *rab27a*: BDE-47_{0.312 mg/L} and BDE-47_{0.625 mg/L}: $P < 0.001$; Fig. 7d, *mlpha*: BDE-47_{0.625 mg/L} $P < 0.05$, BDE-47_{1.250 mg/L}: $P < 0.01$; Fig. 7e, *cdc42*: BDE-47_{1.250 mg/L} $P < 0.05$; versus control group). As shown in Fig. 7f–j, when the embryos were 72 hpf old, gene expression of *myosin VAa*, *kif5ba*, and *mlpha* was decreased in 0.312 and 1.250 mg/L groups ($P < 0.001$; versus control group), and the transcription levels of *rab27a* were decreased in all BDE-47 treated groups ($P < 0.001$; versus control group). The expression of cell division cycle 42 (*cdc42*) was inhibited in 0.312 mg/L or 1.250 mg/L BDE-47 group ($P < 0.001$; versus control group), but was abnormally enhanced in 0.625 mg/L BDE-47 group ($P < 0.05$; versus control group).

Discussion

This study assessed the neurotoxic effects of BDE-47 during zebrafish development (Fig. 8). Zebrafish coiling has been taken as a rapid and sensitive endpoint for neurotoxicity evaluation (Wang et al. 2018; Zheng et al. 2021). Several previous studies have established that BDE-47 exposure can stimulate zebrafish embryo coiling (Usenko et al. 2011; Chen et al. 2012; Tanaka et al. 2018). Consistently, our results in this study supported BDE-47 exposure evoked embryo coiling behavior at 1.250 mg/L by 24 hpf. Moreover, we revealed a novel inhibitory effect of BDE-47 on skin pigmentation. BDE-47 reduced melanin presence at the dorsal regions of the head and yolk sac at concentrations of 0.625 and 1.250 mg/L. PBDE concentrations in nature's water

environment were generally low because they have high octanol/water partition coefficient values (Wang et al. 2021). But higher BDE-47 concentrations were required to induce phenotype changes in zebrafish during the developmental period. It has been confirmed the bioaccumulated PBDEs levels in zebrafish embryos following semi-static waterborne exposure (BDE-47 0.5–5 mg/L; DE-71 100 μ g/L) fell into the same range as those environmental and human samples (Lema et al. 2007; Chen et al. 2012; Wang et al. 2022), suggesting the concentrations used in this study can generate a similar body burden relevant to environmental samples.

We then performed biochemical and protein expression assays to explore the potential mechanisms of BDE-47-induced neurobehavior changes in 24 hpf embryos. The dopamine system is an important target of PBDEs (Wang et al. 2016). In this study, dopamine level was increased by 1.250 mg/L BDE-47. Other study revealed dopamine content declined in zebrafish after exposure to 1 mg/L BDE-47 from 57 to 60 hpf (Tanaka et al. 2018). Since zebrafish dopaminergic neurons emerge at about 22 hpf, we presume the effect of BDE-47 on dopamine production is complicated and possibly related with other factors, such as exposure timing and duration. The 5-HT level was also enhanced by BDE-47 in this study, which is in line with the finding in the mice model (Ji et al. 2019b). A disrupted 5-HT system was implicated in abnormal zebrafish coiling behavior (Wang et al. 2018), thus we presume that increased 5-HT may be a cause of BDE-47-induced neurotoxicity. As a neural stem/progenitor cell marker, nestin is required for the survival, renewal, and proliferation of neural progenitor cells (Park et al. 2010). We found BDE-47 significantly decreased embryos' nestin

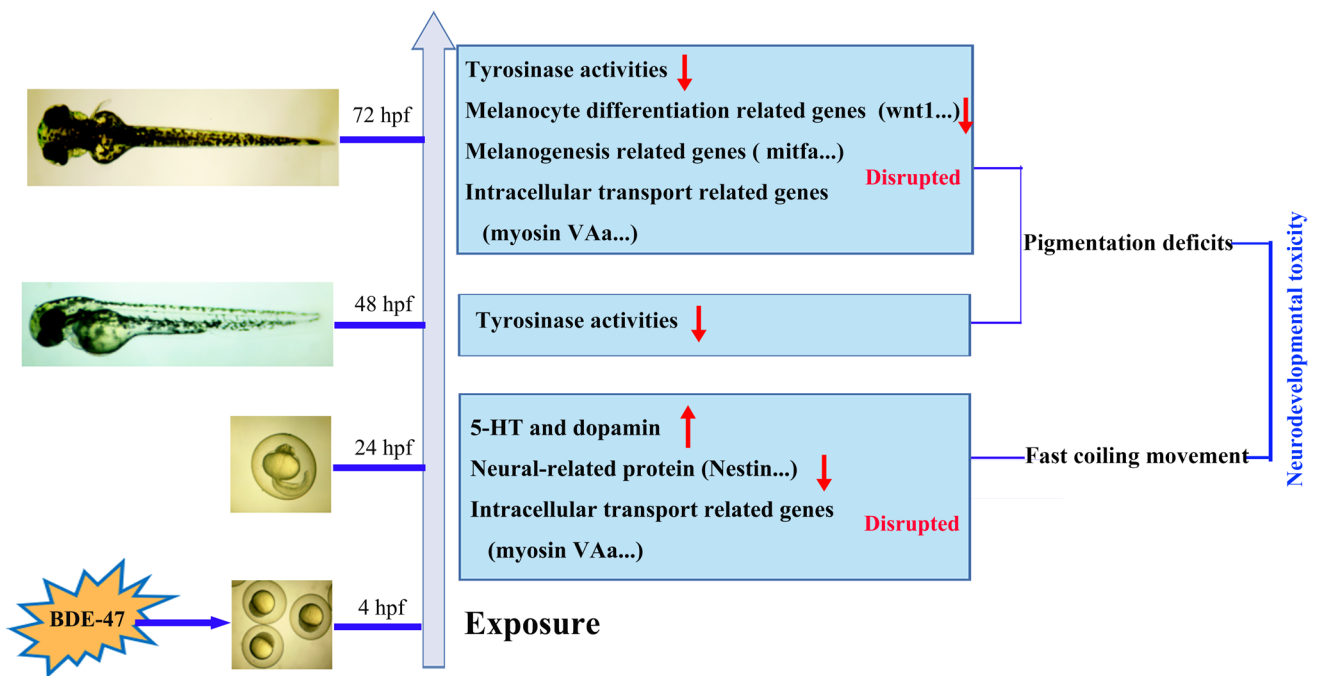


Fig. 8 Schematic diagram of neurobehavioral and morphological toxicity phenotypes and mechanisms of BDE-47 during zebrafish development

levels, indicating the early development procedure such as proliferation and differentiation of neural stem/progenitor cells may be inhibited. Gap43, PSD95, and GFAP are well-known markers for the nervous system that are critical for neurodevelopment, and they are common molecular targets of BDE-47 (Wang et al. 2011; Dingemans et al. 2007; Kodavanti et al. 2015). Similarly, we found BDE-47 descended their expression in 24 hpf embryos, suggesting the embryos' neurogenesis was also disturbed. Though previous toxicological data established BDE-47 evoked fast coiling in zebrafish before 27 hpf, the mechanism was usually investigated later (such as at 48 hpf, 72 hpf or 128 hpf) (Tanaka et al. 2018; Wang et al. 2018; Zheng et al. 2021). Here, our results obtained from the 24 hpf zebrafish embryos will provide additional information for the neurotoxicity of BDE-47.

The neural crest is a population of cells arising from the dorsal neural tube that develop initially in parallel with central nervous system precursors and then generate a variety of cell types, including neurons and glia of the peripheral nervous system and pigment cells. Neural crest has been long utilized for neurodevelopmental toxicity testing of various environmental chemicals (Zimmer et al. 2012). Zebrafish neural crest produces three distinct kinds of pigment cells, and melanocytes are the first to appear in embryos for melanin synthesis. Melanocytes share a common embryologic origin, signaling molecules, and pathways with the nervous system neurons, and the similarities make melanocytes an attractive model system for neurological disease investigation (Yaar and Park, 2012; Wang et al. 2020). Transcription

factor *mitf*, by regulating the transcription of *tyrosinase* and *tyrp*, functions as a master regulator of multiple molecular cascades that control melanocyte survival, proliferation, and melanogenesis (Cheli et al. 2010). In zebrafish embryos, *mitf* ortholog *mitfa* is transcriptionally activated by *sox10* via binding directly to its promoter in neural crest cells (Elworthy et al. 2003). Functionally, *wnt* signaling, especially *wnt1* and *wnt3* signaling, can facilitate the differentiation of neural crest cells into melanocytes through the induction of *mitf* expression (Dorsky et al. 1998). The biosynthesis of melanin was critically regulated via a tyrosinase-dependent way, during which tyrosinase serves as a rate-limiting enzyme and acts with *tyrp1* and *tyrp2* to promote melanogenesis (Olivares and Solano, 2009). As a strong determinant of the eumelanin content in melanocytes, *oca2* modulates the activity of tyrosinase (Manga et al. 2001). Here, BDE-47 descended zebrafish tyrosinase activity, but did not affect the mushroom tyrosinase activity, suggesting BDE-47 inhibited zebrafish tyrosinase activity in an indirect manner. Moreover, BDE-47 restrained expression of *wnt1*, *wnt3*, *sox10*, *tyrp1b*, *tyrp2*, and *oca2* genes in 72 hpf embryos. Though the effects of BDE-47 concentrations on the transcriptional activity of *mitfa* and *tyrp1a* were complicated, their protein levels were decreased by BDE-47 in zebrafish embryos (Supplementary Fig. 1). These alternations might be the potential reasons for melanin accumulation deficits in zebrafish embryos and increased gene expression of *mitfa* and *tyrp1a* in 0.625 mg/L BDE-47 group may be a compensatory mechanism for defective melanogenesis. To

date, there is little literature available concerning the effects of PBDEs on neural crest-derived melanocyte. Our results clearly indicated BDE-47 hindered melanocyte development and melanin biosynthesis, which may extend our understanding of the neurotoxicity of PBDEs. Because zebrafish melanocytes become distinguishable beginning at approximately 24 hpf (Lister, 2002), we also determined the gene expression described above in 24 hpf zebrafish. However, no significant changes were observed (except *wnt1*) (data not shown), indicating that BDE-47 affected melanocyte development and melanogenesis mainly at 72 hpf.

Myosin VA and *kif5b* are the two most prevalent motor proteins in nerve cells and melanocytes, responsible for actin- and microtubule-dependent transport, respectively. Myosin VA-mediated trafficking contributed to the dendritic architecture and excitatory synapse development (Ultanir et al. 2014; Lisé et al. 2009; Yoshii et al. 2013). In melanocytes, myosin VA expression inhibition resulted in fewer and shorter dendritic processes in appearance (Edgar and Bennett, 1999), suggesting the involvement of myosin VA in establishing the dendritic morphology of melanocytes. *Kif5b*-mediated transport is critical for neuronal developmental processes, such as neuronal polarity (Jacobson et al. 2006), presynaptic assembly and synaptogenesis (Cai et al. 2007), and synaptic plasticity (Zhao et al. 2020). It is also known that myosin VA and *kif5b* are essential for melanosome dispersion (Wu et al. 2002; Hara et al. 2000). Following melanin biogenesis, *Kif5b* regulates outward melanosome transport along microtubules, while Myosin VA, *mlpha*, and *Rab27a* form a ternary complex to drive the movement of melanosomes along actin filaments towards the cell extensions (Wu et al. 2002). Besides, *Cdc42* regulates dendritic and axonal morphogenesis in neural cells (Scott et al. 2003; Schwamborn and Püschel, 2004). It also functions in melanocyte morphology and melanosome transfer (Ando et al. 2012). Our results revealed that at 24 hpf, BDE-47 markedly enhanced the expression of *myosin VAa*, *rab27a*, *mlpha*, and *cdc42*, whereas the expression of *kif5ba* was unchanged significantly. These up-regulations may be stress responses of the body to keep normal actin-based transport process to the noxious stimulation. At 72 hpf, the transcription of *myosin VAa*, *kif5ba*, *rab27a*, and *mlpha* were inhibited by BDE-47. Though the gene expression of *cdc42* was complicated, its protein level was decreased due to BDE-47 exposure (Supplementary Fig. 1). These findings suggested the intracellular transport process was disrupted by BDE-47, and the actin-based transport process was impacted prior to the microtubule-dependent transport. Together with a recent report showing the inhibitory effects of BDE-47 on the dendritic length and pine density of the prefrontal cortex (Li et al. 2021), we would like to propose that disturbed intracellular transport process might ultimately affect cell morphogenesis, synaptic plasticity, and melanosome dispersion, which may be a potential explanation for the neurobehavioral

abnormalities and pigmentation deficit in zebrafish embryos during development.

In fish melanophores, melanosomes can either aggregate around the cell centre or disperse uniformly throughout the cell. Previous studies suggested the melanosomes aggregate impacts fish skin color in the developmental stage (Mueller and Neuhauss, 2014), and whether the melanosomes aggregate process was also disrupted by BDE-47 is still unknown. Although the biochemical and molecular changes in zebrafish have been investigated, the direct evidence for phenotypic changes of central or peripheral nervous system was not provided. These are limitations of this study, which are worthy of further investigation.

Conclusion

In the present study, zebrafish was utilized to explore the phenotypes and mechanisms underlying neurodevelopmental disorders of BDE-47. These results offer new insights into the neurodevelopmental toxicity of PBDE and facilitate the comprehensive evaluation of neurotoxicity in embryos.

Supplementary Information The online version contains supplementary material available at <https://doi.org/10.1007/s11356-023-26170-7>.

Author contribution All authors contributed to the study conception and design. Material preparation, data collection, and analysis were performed by Hui Liang, Wen-feng Zhang, and Ze-yu Sun. Ying Qin and Han-bo Shi participated in the data analysis. Juan Zhuang conceived and designed the experimentation, supervised the work and written the first draft of the manuscript. All authors commented on previous versions of the manuscript. Zheng Jun-pan reviewed and revised the manuscript. All authors read and approved the final manuscript.

Funding This research was supported by the University Natural Science Foundation of Jiangsu Province (18KJB330001); the Industry-University-Research Cooperation Project of Jiangsu Province, China (BY2021394).

Data availability The datasets used and/or analyzed during the current study are available from the corresponding author on reasonable request.

Declarations

Ethics approval Not applicable.

Consent to participate Not applicable.

Consent for publication Not applicable.

Competing interests The authors declare no competing interests.

References

- Abbasi G, Buser AM, Soehl A, Murray MW, Diamond ML (2015) Stocks and flows of PBDEs in products from use to waste in

- the US and Canada from 1970 to 2020. *Environ Sci Technol* 49(3):1521–1528. <https://doi.org/10.1021/es504007v>
- Ando H, Niki Y, Ito M, Akiyama K, Matsui MS, Yarosh DB, Ichihashi M (2012) Melanosomes are transferred from melanocytes to keratinocytes through the processes of packaging, release, uptake, and dispersion. *J Invest Dermatol* 132(4):1222–1229. <https://doi.org/10.1038/jid.2011.413>
- Azar N, Booij L, Muckle G, Arbuckle TE, Séguin JR, Asztalos E, Fraser WD, Lanphear BP, Bouchard MF (2021) Prenatal exposure to polybrominated diphenyl ethers (PBDEs) and cognitive ability in early childhood. *Environ Int* 146:106296. <https://doi.org/10.1016/j.envint.2020.106296>
- Blanc M, Alfonso S, Bégout ML, Barrachina C, Hyötyläinen T, Keiter SH, Cousin X (2021) An environmentally relevant mixture of polychlorinated biphenyls (PCBs) and polybrominated diphenylethers (PBDEs) disrupts mitochondrial function, lipid metabolism and neurotransmission in the brain of exposed zebrafish and their unexposed F2 offspring. *Sci Total Environ* 754:142097. <https://doi.org/10.1016/j.scitotenv.2020.142097>
- Blanco J, Mulero M, Heredia L, Pujol A, Domingo JL, Sánchez DJ (2013) Perinatal exposure to BDE-99 causes learning disorders and decreases serum thyroid hormone levels and BDNF genes expression in hippocampus in rat offspring. *Toxicology* 308:122–128. <https://doi.org/10.1016/j.tox.2013.03.010>
- Brustein E, Chong M, Holmqvist B, Drapeau P (2003) Serotonin patterns locomotor network activity in the developing zebrafish by modulating quiescent periods. *J Neurobiol* 57(3):303–322. <https://doi.org/10.1002/neu.10292>
- Burgoyne T, O'Connor MN, Seabra MC, Cutler DF, Futter CE (2015) Regulation of melanosome number, shape and movement in the zebrafish retinal pigment epithelium by OA1 and PMEL. *J Cell Sci* 128(7):1400–1407. <https://doi.org/10.1242/jcs.164400>
- Cai K, Song Q, Yuan W, Yang G, Li J (2022) Composition changes, releases, and potential exposure risk of PBDEs from typical E-waste plastics. *J Hazard Mater* 424:127227. <https://doi.org/10.1016/j.jhazmat.2021.127227>
- Cai Q, Pan PY, Sheng ZH (2007) Syntabulin-kinesin-1 family member 5B-mediated axonal transport contributes to activity-dependent presynaptic assembly. *J Neurosci* 27(27):7284–7296. <https://doi.org/10.1523/JNEUROSCI.0731-07.2007>
- Cheli Y, Ohanna M, Ballotti R, Bertolotto C (2010) Fifteen-year quest for microphthalmia-associated transcription factor target genes. *Pigment Cell Melanoma Res* 23(1):27–40. <https://doi.org/10.1111/j.1755-148X.2009.00653.x>
- Chen J, Li X, Li X, Chen D (2018) The environmental pollutant BDE-209 regulates NO/cGMP signaling through activation of NMDA receptors in neurons. *Environ Sci Pollut Res* 25(4):3397–3407. <https://doi.org/10.1007/s11356-017-0651-5>
- Chen X, Huang C, Wang X, Chen J, Bai C, Chen Y, Dong Q, Yang D (2012) BDE-47 disrupts axonal growth and motor behavior in developing zebrafish. *Aquat Toxicol* 120:121:35–44. <https://doi.org/10.1016/j.aquatox.2012.04.014>
- Costa LG, Pellacani C, Dao K, Kavanagh TJ, Roque PJ (2015) The brominated flame retardant BDE-47 causes oxidative stress and apoptotic cell death in vitro and in vivo in mice. *Neurotoxicology* 48:68–76. <https://doi.org/10.1016/j.neuro.2015.03.008>
- Ding G, Yu J, Cui C, Chen L, Gao Y, Wang C, Zhou Y, Tian Y (2015) Association between prenatal exposure to polybrominated diphenyl ethers and young children's neurodevelopment in China. *Environ Res* 142:104–111. <https://doi.org/10.1016/j.envres.2015.06.008>
- Dingemans MM, Ramakers GM, Gardoni F, van Kleef RG, Bergman A, Di Luca M, van den Berg M, Westerink RH, Vijverberg HP (2007) Neonatal exposure to brominated flame retardant BDE-47 reduces long-term potentiation and postsynaptic protein levels in mouse hippocampus. *Environ Health Perspect* 115(6):865–870. <https://doi.org/10.1289/ehp.9860>
- Dorsky RI, Moon RT, Raible DW (1998) Control of neural crest cell fate by the Wnt signalling pathway. *Nature* 396(6709):370–373. <https://doi.org/10.1038/24620>
- Drobná B, Fabišková A, Čonka K, Gago F, Oravcová P, Wimmerová S, Oktapodas Feiler M, Šovčíková E (2019) PBDE serum concentration and preschool maturity of children from Slovakia. *Chemosphere* 233:387–395. <https://doi.org/10.1016/j.chemosphere.2019.05.284>
- Edgar AJ, Bennett JP (1999) Inhibition of dendrite formation in mouse melanocytes transiently transfected with antisense DNA to myosin Va. *J Anat* 195(Pt 2):173–184. <https://doi.org/10.1046/j.1469-7580.1999.19520173.x>
- Elworthy S, Lister JA, Carney TJ, Raible DW, Kelsh RN (2003) Transcriptional regulation of mitfa accounts for the sox10 requirement in zebrafish melanophore development. *Development* 130(12):2809–2818. <https://doi.org/10.1242/dev.00461>
- Eskenazi B, Chevrier J, Rauch SA, Kogut K, Harley KG, Johnson C, Trujillo C, Sjödin A, Bradman A (2013) In utero and childhood polybrominated diphenyl ether (PBDE) exposures and neurodevelopment in the CHAMACOS study. *Environ Health Perspect* 121(2):257–262. <https://doi.org/10.1289/ehp.1205597>
- Hara M, Yaar M, Byers HR, Goukassian D, Fine RE, Gonsalves J, Gilchrist BA (2000) Kinesin participates in melanosomal movement along melanocyte dendrites. *J Invest Dermatol* 114(3):438–443. <https://doi.org/10.1046/j.1523-1747.2000.00894.x>
- Hou L, Jiang J, Gan Z, Dai YY, Yang P, Yan Y, Ding S, Su S, Bao X (2019) Spatial distribution of organophosphorus and brominated flame retardants in surface water, sediment, groundwater, and wild fish in chengdu, china. *Arch Environ Contam Toxicol* 77:279–290. <https://doi.org/10.1007/s00244-019-00624-x>
- Jacobson C, Schnapp B, Banker GA (2006) A change in the selective translocation of the kinesin-1 motor domain marks the initial specification of the axon. *Neuron* 49(6):797–804. <https://doi.org/10.1016/j.neuron.2006.02.005>
- Ji F, Sreenivasamurthy SG, Wei J, Shao X, Luan H, Zhu L, Song J, Liu L, Li M, Cai Z (2019b) Study of BDE-47 induced Parkinson's disease-like metabolic changes in C57BL/6 mice by integrated metabolomic, lipidomic and proteomic analysis. *J Hazard Mater* 378:120738. <https://doi.org/10.1016/j.jhazmat.2019.06.015>
- Ji H, Liang H, Wang Z, Miao M, Wang X, Zhang X, Wen S, Chen A, Sun X, Yuan W (2019a) Associations of prenatal exposures to low levels of polybrominated diphenyl ether (PBDE) with thyroid hormones in cord plasma and neurobehavioral development in children at 2 and 4 years. *Environ Int* 131:105010. <https://doi.org/10.1016/j.envint.2019.105010>
- Kodavanti PR, Royland JE, Osorio C, Winnik WM, Ortiz P, Lei L, Ramabhadran R, Alzate O (2015) Developmental exposure to a commercial PBDE mixture: effects on protein networks in the cerebellum and hippocampus of rats. *Environ Health Perspect* 123(5):428–436. <https://doi.org/10.1289/ehp.1408504>
- Labunska I, Harrad S, Santillo D, Johnston P, Brigden K (2013) Levels and distribution of polybrominated diphenyl ethers in soil, sediment and dust samples collected from various electronic waste recycling sites within Guiyu town, southern China. *Environ Sci: Processes Impacts* 15(2):503–511. <https://doi.org/10.1039/c2em30785e>
- Labunska I, Harrad S, Wang M, Santillo D, Johnston P (2014) Human dietary exposure to PBDEs around e-waste recycling sites in Eastern China. *Environ Sci Technol* 48:5555–5564. <https://doi.org/10.1021/es500241m>
- Lema SC, Schultz IR, Scholz NL, Incardona JP, Swanson P (2007) Neural defects and cardiac arrhythmia in fish larvae following embryonic exposure to 2, 2', 4, 4'-tetrabromodiphenyl ether

- (PBDE 47). *Aquat Toxicol* 82(4):296–307. <https://doi.org/10.1016/j.aquatox.2007.03.002>
- Li N, Chen XW, Deng WJ, Giesy JP, Zheng HL (2018) PBDEs and dechlorane plus in the environment of Guiyu, Southeast China: a historical location for E-waste recycling (2004, 2014). *Chemosphere* 199:603–611. <https://doi.org/10.1016/j.chemosphere.2018.02.041>
- Li Z, You M, Che X, Dai Y, Xu Y, Wang Y (2021) Perinatal exposure to BDE-47 exacerbated autistic-like behaviors and impairments of dendritic development in a valproic acid-induced rat model of autism. *Ecotoxicol Environ Saf* 212:112000. <https://doi.org/10.1016/j.ecoenv.2021.112000>
- Liang H, Vuong AM, Xie C, Webster GM, Sjödin A, Yuan W, Miao M, Braun JM, Dietrich KN, Yolton K, Lanphear BP, Chen A (2019) Childhood polybrominated diphenyl ether (PBDE) serum concentration and reading ability at ages 5 and 8 years: the HOME Study. *Environ Int* 122:330–339. <https://doi.org/10.1016/j.envint.2018.11.026>
- Lin C, Zeng Z, Xu R, Liang W, Guo Y, Huo X (2022) Risk assessment of PBDEs and PCBs in dust from an e-waste recycling area of China. *Sci Total Environ* 803:150016. <https://doi.org/10.1016/j.scitotenv.2021.150016>
- Lindberg P, Sellstrom U, Haggberg L, de Wit CA (2004) Higher brominated diphenyl ethers and hexabromocyclododecane found in eggs of peregrine falcons (*Falco peregrinus*) breeding in Sweden. *Environ Sci Tech* 38:93e96. <https://doi.org/10.1021/es034614q>
- Lisé MF, Srivastava DP, Arstikaitis P, Lett RL, Sheta R, Viswanathan V, Penzes P, O'Connor TP, El-Husseini A (2009) Myosin-Va-interacting protein, RILPL2, controls cell shape and neuronal morphogenesis via Rac signaling. *J Cell Sci* 122(20):3810–3821. <https://doi.org/10.1242/jcs.050344>
- Lister JA (2002) Development of pigment cells in the zebrafish embryo. *Microsc Res Tech* 58(6):435–441. <https://doi.org/10.1002/jemt.10161>
- Liu D, Xue D, Lu W, Yang Z, Li L, Xia B, Wei J, Chen X, Yang Y, Wang X, Lin G (2022) BDE-47 induced PC-12 cell differentiation via TrkA downstream pathways and caused the loss of hippocampal neurons in BALB/c mice. *J Hazard Mater* 422:126850. <https://doi.org/10.1016/j.jhazmat.2021.126850>
- Liu W, Wang M, Xu S, Gao C, Liu J (2019) Inhibitory effects of shell of *Camellia oleifera* Abel extract on mushroom tyrosinase and human skin melanin. *J Cosmet Dermatol* 18(6):1955–1960. <https://doi.org/10.1111/jocd.12921>
- Manga P, Boissy RE, Pifko-Hirst S, Zhou BK, Orlow SJ (2001) Mislocalization of melanosomal proteins in melanocytes from mice with oculocutaneous albinism type 2. *Exp Eye Res* 72:695–710. <https://doi.org/10.1111/pcmr.12210>
- Mueller KP, Neuhauss SCF (2014) Sunscreen for fish: co-option of UV light protection for camouflage. *PLoS One* 9(1):e87372. <https://doi.org/10.1371/journal.pone.0087372>
- Olivares C, Solano F (2009) New insights into the active site structure and catalytic mechanism of tyrosinase and its related proteins. *Pigment Cell Melanoma Res* 22(6):750–760. <https://doi.org/10.1111/j.1755-148X.2009.00636.x>
- Park D, Xiang AP, Mao FF, Zhang L, Di CG, Liu XM, Shao Y, Ma BF, Lee JH, Ha KS, Walton N, Lahn BT (2010) Nestin is required for the proper self-renewal of neural stem cells. *Stem Cells* 28(12):2162–2171. <https://doi.org/10.1002/stem.541>
- Ramlan NF, Sata NSAM, Hassan SN, Bakar NA, Ahmad S, Zulkifli SZ, Abdullah CAC, Ibrahim WNW (2017) Time dependent effect of chronic embryonic exposure to ethanol on zebrafish: morphology, biochemical and anxiety alterations. *Behav Brain Res* 332:40–49. <https://doi.org/10.1016/j.bbr.2017.05.048>
- Schwamborn JC, Püschel AW (2004) The sequential activity of the GTPases Rap1B and Cdc42 determines neuronal polarity. *Nat Neurosci* 7(9):923–929. <https://doi.org/10.1038/nn1295>
- Scott EK, Reuter JE, Luo L (2003) Small GTPase Cdc42 is required for multiple aspects of dendritic morphogenesis. *J Neurosci* 23(8):3118–3123. <https://doi.org/10.1523/jneurosci.23-08-03118.2003>
- Tanaka Y, Fujiwara M, Shindo A, Yin G, Kitazawa T, Teraoka H (2018) Aroclor 1254 and BDE-47 inhibit dopaminergic function manifesting as changes in locomotion behaviors in zebrafish embryos. *Chemosphere* 193:1207–1215. <https://doi.org/10.1016/j.chemosphere.2017.11.138>
- Thirumalai V, Cline HT (2008) Endogenous dopamine suppresses initiation of swimming in prefeeding zebrafish larvae. *J Neurophysiol* 100(3):1635–1648. <https://doi.org/10.1152/jn.90568.2008>
- Ultanir SK, Yadav S, Hertz NT, Osés-Prieto JA, Claxton S, Burlingame AL, Shokat KM, Jan LY, Jan YN (2014) MST3 kinase phosphorylates TAO1/2 to enable Myosin Va function in promoting spine synapse development. *Neuron* 84(5):968–982. <https://doi.org/10.1016/j.neuron.2014.10.025>
- Usenko CY, Robinson EM, Usenko S, Brooks BW, Bruce ED (2011) PBDE developmental effects on embryonic zebrafish. *Environ Toxicol Chem* 30(8):1865–1872. <https://doi.org/10.1002/etc.570>
- Varshavsky JR, Robinson JF, Zhou Y, Puckett KA, Kwan E, Buarprung S, Aburajab R, Gaw SL, Sen S, Smith SC, Frankenfield J, Park JS, Fisher SJ, Woodruff TJ (2020) Association of polybrominated diphenyl ether (PBDE) levels with biomarkers of placental development and disease during mid-gestation. *Environ Health* 19:1–16. <https://doi.org/10.1186/s12940-020-00617-7>
- Wang F, Fang M, Hinton DE, Chernick M, Jia S, Zhang Y, Xie L, Dong W, Dong W (2018) Increased coiling frequency linked to apoptosis in the brain and altered thyroid signaling in zebrafish embryos (*Danio rerio*) exposed to the PBDE metabolite 6-OH-BDE-47. *Chemosphere* 198:342–350. <https://doi.org/10.1016/j.chemosphere.2018.01.081>
- Wang F, Liu W, Jin Y, Dai J, Zhao H, Xie Q, Liu X, Yu W, Ma J (2011) Interaction of PFOS and BDE-47 co-exposure on thyroid hormone levels and TH-related gene and protein expression in developing rat brains. *Toxicol Sci* 121(2):279–291. <https://doi.org/10.1093/toxsci/kfr068>
- Wang H, Meng Z, Liu F, Zhou L, Su M, Meng Y, Zhang S, Liao X, Cao Z, Lu H (2020) Characterization of boscalid-induced oxidative stress and neurodevelopmental toxicity in zebrafish embryos. *Chemosphere* 238:124753. <https://doi.org/10.1016/j.chemosphere.2019.124753>
- Zimmer B, Lee G, Balmer NV, Meganathan K, Sachinidis A, Studer L, Leist M (2012) Evaluation of developmental toxicants and signaling pathways in a functional test based on the migration of human neural crest cells. *Environ Health Perspect* 120(8):1116–1122. <https://doi.org/10.1289/ehp.1104489>
- Wang J, Yan Z, Zheng X, Wang S, Fan J, Sun Q, Xu J, Men S (2021) Health risk assessment and development of human health ambient water quality criteria for PBDEs in China. *Sci Total Environ* 799:149353. <https://doi.org/10.1016/j.scitotenv.2021.149353>
- Wang X, Yang L, Wang Q, Guo Y, Li N, Ma M, Zhou B (2016) The neurotoxicity of DE-71: effects on neural development and impairment of serotonergic signaling in zebrafish larvae. *J Appl Toxicol* 36(12):1605–1613. <https://doi.org/10.1002/jat.3322>
- Wang X, Zhao L, Shi Q, Guo Y, Hua J, Han J, Yang L (2022) DE-71 affected the cholinergic system and locomotor activity via disrupting calcium homeostasis in zebrafish larvae. *Aquat Toxicol* 250:106237. <https://doi.org/10.1016/j.aquatox.2022.106237>
- Wu XS, Rao K, Zhang H, Wang F, Sellers JR, Matesic LE, Copeland NG, Jenkins NA, Hammer JA 3rd (2002) Identification of an organellar receptor for myosin-Va. *Nat Cell Biol* 4(4):271–278. <https://doi.org/10.1038/ncb760>
- Yaar M, Park HY (2012) Melanocytes: a window into the nervous system. *J Invest Dermatol* 132(3):835–845. <https://doi.org/10.1038/jid.2011.386>

- Yoshii A, Zhao JP, Pandian S, van Zundert B, Constantine-Paton M (2013) A myosin Va mutant mouse with disruptions in glutamate synaptic development and mature plasticity in visual cortex. *J Neurosci* 33(19):8472–8482. <https://doi.org/10.1523/JNEUROSCI.4585-12.2013>
- Zhao J, Fok AHK, Fan R, Kwan PY, Chan HL, Lo LH, Chan YS, Yung WH, Huang J, Lai CSW, Lai KO (2020) Specific depletion of the motor protein KIF5B leads to deficits in dendritic transport, synaptic plasticity and memory. *Elife* 9:e53456. <https://doi.org/10.7554/eLife.53456>
- Zheng S, Huang W, Liu C, Xiao J, Wu R, Wang X, Cai Z, Wu K (2021) Behavioral change and transcriptomics reveal the effects of 2, 2', 4, 4'-tetrabromodiphenyl ether exposure on neurodevelopmental

toxicity to zebrafish (*Danio rerio*) in early life stage. *Sci Total Environ* 752:141783. <https://doi.org/10.1016/j.scitotenv.2020.141783>

Publisher's note Springer Nature remains neutral with regard to jurisdictional claims in published maps and institutional affiliations.

Springer Nature or its licensor (e.g. a society or other partner) holds exclusive rights to this article under a publishing agreement with the author(s) or other rightsholder(s); author self-archiving of the accepted manuscript version of this article is solely governed by the terms of such publishing agreement and applicable law.